LOAD VOLTAGE REGULATION VIA TRANSMITTER POWER SUPPLY CONTROL FOR WIRELESSLY POWERED BIOMEDICAL IMPLANTS

By

NABIL MOHAMMAD

A thesis submitted to the

Graduate School-New Brunswick

Rutgers, The State University of New Jersey

In partial fulfillment of the requirements

For the degree of

Masters of Science

Graduate Program in Electrical and Computer Engineering

Written under the direction of

Dr. Laleh Najafizadeh

And approved by

_____

_____

_____

New Brunswick, New Jersey

January 2017

ABSTRACT OF THESIS

Load Voltage Regulation via Transmitter Power Supply Control for Wirelessly Powered Biomedical Implants

by Nabil Mohammad

Thesis Director: Dr. Laleh Najafizadeh

Wireless power transfer (WPT) via inductive links has been an attractive solution for powering biomedical implants. Due to the nature of the human body (e.g. body movement or changes in the biological environment), however, the transmitter (TX) and receiver (RX) coils involved in WPT are prone to misalignment, causing variations in the coupling factor. The variation in the coupling factor results in variations in the voltage that is delivered to the load on the receiver end.

A solution to the problem of load voltage variation is to employ negative feedback on the transmitter end. Towards this goal, a feedback control architecture is proposed for the regulation of the load voltage under coupling variations. It is shown that by controlling the power supply on the transmitter end, through voltage-mode feedback control, the load voltage can be regulated. In the design of the controller, the open-loop system of the power control unit and WPT system have been taken into consideration. Theoretical derivations are presented and the validity of the proposed concept is investigated using simulations.

Acknowledgement

First and foremost, I would like to thank my parents, Rashida and Vaseem, for instilling motivation in me to pursue great yet difficult endeavors with diligence and fortitude. It has been a long journey getting to where I am now; if it wasn't for their commitment and guidance, I would have not been thriving in the way I am today. I would also like to thank my friends for putting up with my constant venting over the past year as a graduate student and their unconditional love and encouragement to keep me going.

I would like to thank my thesis advisor, Dr. Laleh Najafizadeh for her patience and encouragement over the past year. Her advice and rigorous expectations eventually led me to actively broaden my knowledge above what I had expected of myself coming into graduate school, and for this I am very grateful.

My special thanks to Dr. Michael Caggiano who enthusiastically conveyed engineering practicality amongst a curriculum muddled with theory and no play. I will always remember his teachings throughout my professional career as an engineer and recreational leisure as an electronics hobbyist. My sincere gratitude goes to him.

And lastly, I would also like to thank Dr. Mehdi Javanmard and, again, Dr. Michael Caggiano for volunteering to be part of the committee.

Table of Content

List of Tables

List of Figures

Chapter 1
Introduction

Ever since the rise of electronic biomedical implants, one of the many primary challenges faced by engineers and scientists was maintaining the implanted device's battery life or power level. It is obvious that once a patient's device implant runs out power, it would be a nuance to repeatedly have to perform the surgery to replace the battery; as this would be costly, inconvenient and pestering to the patient's well-being. Clearly, an ideal solution would be without having to tamper with the body at all, and this is where the wireless power transfer (WPT) technique comes into play.

Wireless power transfer is typically achieved using non-radiative techniques such as inductive coupling between coils of wire, or capacitive coupling between electrodes [1]. In either case, the coupling between the transfer links introduces a wide range of complexities since it's this coupling factor that directly affects a WPT system's ability to perform robustly and efficiently. Biomedical implants typically rely on inductive coupling to transfer power through the skin, meaning that the implant is integrated with a receiver coil that receives power via magnetics fields generated by the transmitter placed outside the body. But due to the dynamic nature of the human body (muscle movements or misplacement), these coils are prone to misalignment and therefore their coupling, denoted as a coefficient k, will not be stable. This coupling variation leads to voltage variation across the receiver coil and directly impacts the power delivered to the load. A widely used method to combat this issue is to integrate feedback through wireless communication

links or telemetry [2], [3], [4], [12], [22], and [23]; the load voltage is detected and sent to the transmitter-side as a feedback signal. With this feedback signal, a controller can determine whether to increase or decrease the power emitted from the transmitter and eventually regulate the load voltage. Not only does the misalignment affect the load voltage, but also effects the performance of the WPT system. Typical WPT structures utilize a class-E amplifier to drive the transmitter coil because of their high efficiency [6]. But because the amplifier's optimal condition relies highly on the impedance of the load network, any variations in the mutual coupling between the coils can cause the amplifier to operate in non-optimal conditions, leading to power loss. To combat this, parameters such as operating frequency, duty-cycle, or component value can be tuned to compensate this coil misalignment [3], [5], [9], [10], [11], [25], [26]. Efficiency loss and load voltage regulation are two problems that can be dealt independently using parallel compensation or tuning techniques; in this paper, we will focus load voltage regulation.

1.1 Motivation and research objectives

Coil misalignment can be detrimental if the unit to be powered is for example a pacemaker; if not enough power is available, the device cannot guarantee proper functionality. The methods in [2], [3], [4], [12], [22], and [23] tackle the problem of load voltage regulation by using telemetry to obtain information about the load voltage and accordingly adjust the power amplifier's supply voltage until the desired load voltage level is met. Although the methods introduced are promising, they don't take into account the open-loop transfer function of the power control unit (PCU) or the WPT system in their controller design. The goal of this work is to come up with a robust power supply control architecture that utilizes linear feedback control to compensate for the effect of coil

misalignment on the load voltage. Like all linear controllers, they must be designed based on the open-loop transfer function of the system. Therefore an open-loop transfer function must be obtained, relating the control input of the PCU to the load voltage level on the secondary-side.

1.2 Organization of the thesis

Chapter 2 discusses the operation of the class-E amplifier, its place in WPT systems and previous implementation of power supply control in WPT systems.

In Chapter 3, the proposed power supply control architecture is presented along with analysis regarding obtaining the transfer function of the open-loop system. The design of the controller is also discussed.

In Chapter 4, a simulation model is presented with results validating the open-loop transfer function and demonstrating load voltage regulation.

Chapter 5 concludes the thesis by presenting an overview of contributions and discussing directions for future work.

Chapter 2
Wireless Power Transfer System and Control

Wireless power transfer is a suitable solution for powering biomedical implants. In this chapter, the architecture for a WPT system utilizing a class-E amplifier is presented. The misalignment issue and its effect on power delivery are discussed. And lastly a literature review of the techniques used to compensate the effects of misalignment on the load voltage is also provided.

2.1 Wireless Power Transfer (WPT) System

A wireless power transfer system utilizing inductive coupling links generally consists of a transmitter unit (TX) and a receiver unit (RX). The job of the TX is to convert a battery's DC supply to an AC signal to drive the transmitter coil, inducing a time-varying electromagnetic field. This field is picked up by the receiver coil, inducing a current which is then converted back to DC using rectifier circuitry to power the system on the RX end (e.g. an implant). The structure is shown below in Figure 2.1.

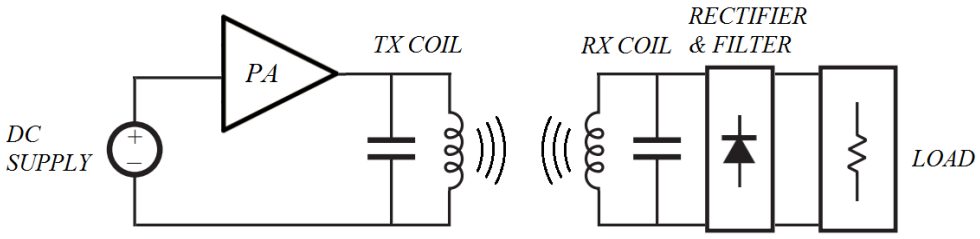

Figure 2.1. Typical structure of a WPT system utilizing inductive coupling links.

The power amplifier (PA) is used to convert DC power to AC power. Typical inverter or switching amplifier topologies used to achieve this conversion are H-bridges, class-D amplifiers, and class-E amplifiers. Switching amplifiers differ from their linear counterparts in that they are highly efficient [6]. In wireless power transfer systems, the class-E amplifier is mostly selected due to the fact it only requires a single transistor. In the following section, the operation of the class-E amplifier will be discussed with the intention of grasping its functionality and place in the WPT structure. The derivation and analysis of its operation can be found in the following references [5] and [6].

2.2 The class-E amplifier

High efficiency amplifiers are notably implemented using switching topologies [27]. The class-E power amplifier (PA), introduced by Sokal [6], is of the switching amplifier family. It is regarded for its high efficiency in converting DC power to AC power. Figure 2.2 illustrates its topology. The MOSFET of the amplifier is typically regarded as an ideal switch with no drain-to-source ON resistance and conducts at a 50% duty cycle at an operating frequency of f_c.

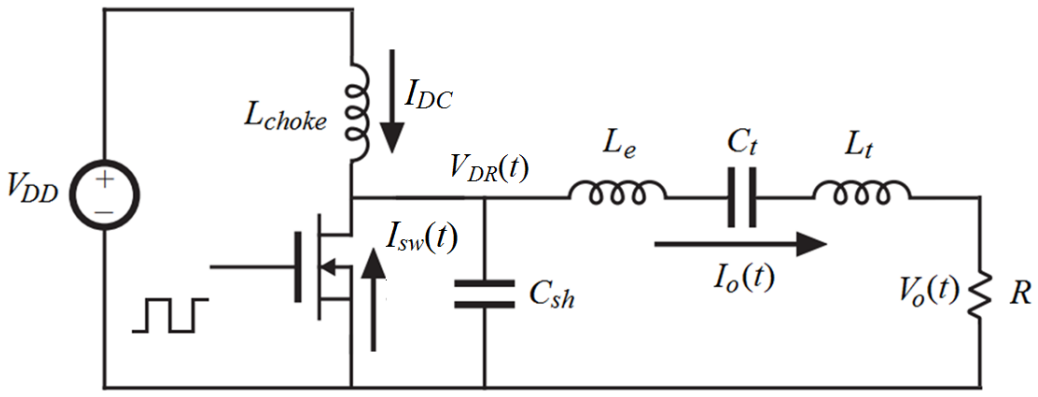

Figure 2.2. Typical configuration of a class-E power amplifier.

Devices acting as switches commonly suffer from efficiency loss due to simultaneous presence of current and voltage during switching transitions between “on” and “off” states. This is due to the intrinsic output capacitor of the MOSFET storing and dissipating energy every switching interval; this switching loss increases linearly with frequency [28]. In this topology the intrinsic output capacitor is absorbed into the shunt capacitor C_{sh}. L_{choke} is seen as an infinite impedance at the operating frequency f_c and all other harmonics so that I_{DC} is ideally a DC current. $I_o(t)$ represents the load current and is purely sinusoidal assuming C_t and L_t form a high Q series resonator at f_c. So the current flowing into the switch-capacitor combination is a sinusoid with a DC offset, denoted as $I_x(t) = I_{DC} + I_o(t)$ [27]. When the switch is off, initially starting at $t = 0$, the current flowing through the switch is zero. When the switch turns on at $t = T_c/2$ (where T_c is the switching period), the current flowing through it can be expressed as

$$I_{sw}(t) = I_x(t) = I_{DC}(1 + a \sin(\omega_c t + \varphi)) \tag{1}$$

where the sinusoidal component is

$$I_o(t) = I_{DC} a \sin(\omega_c t + \varphi)\ . \tag{2}$$

Earlier it was said that during the switch off interval, the switch current is zero; instead $I_x(t)$ will flow entirely into the capacitor C_{sh} and charge it. The voltage across it can be expressed as [27]

$$V_{DR}(t) = \frac{1}{C_{sh}} \int_0^t I_x(t)\, dt\ = \frac{I_{DC}}{\omega_c C_{sh}} (1 + a\,(\cos(\omega_c t + \varphi) - \cos\varphi)). \tag{3}$$

The class-E method is to have the drain-to-source voltage $V_{DR}(t)$ be driven to zero right before the “on” state. From equations (1) and (3), it is evident that $I_{sw}(t)$ and $V_{DR}(t)$

depend on the phase and amplitude of $I_o(t)$. By tuning the load network, the amplitude a, and phase φ, of $I_o(t)$ can be adjusted and a condition can be met where the voltage across C_{sh} is zero prior to the "on" state (4). This condition is known as zero-voltage-switching (ZVS). Not only the voltage but the capacitor current can also be driven to zero to maximally guarantee a zero voltage slope prior to the "on" state (5). These conditions are expressed by

$$V_{DR}\left(t = \frac{T_c}{2}\right) = 0\,, \tag{4}$$

$$\frac{dV_{DR}}{dt}\left(t = \frac{T_c}{2}\right) = 0\,, \tag{5}$$

where T_c is the switching period, $t = 0$ is the initial turn off time and $t = T_c/2$ is the initial turn on time. In [27] it is shown that the value of a and θ needed to manipulate $I_x(t)$ and achieve ZVS, comes out to be

$$a = \sqrt{1 + \frac{\pi^2}{4}}\,, \tag{6}$$

$$\varphi = \tan^{-1}\frac{2}{\pi}\,. \tag{7}$$

Figure 2.3 shows the waveforms of the switch current $I_{sw}(t)$ and $V_{DR}(t)$ under the ZVS condition.

Under ZVS the class-E amplifier has zero switching loss, and assuming there is no conduction loss or parasitic resistances in the passive elements, the amplifier has an efficiency of 100%. This is the main advantage of the class-E switching amplifier over its linear counterparts. The above discussion provides a brief explanation of the operation of

the class-E amplifier; the actual derivations and analysis of the operation of the class E amplifier can be found in [6], [7].

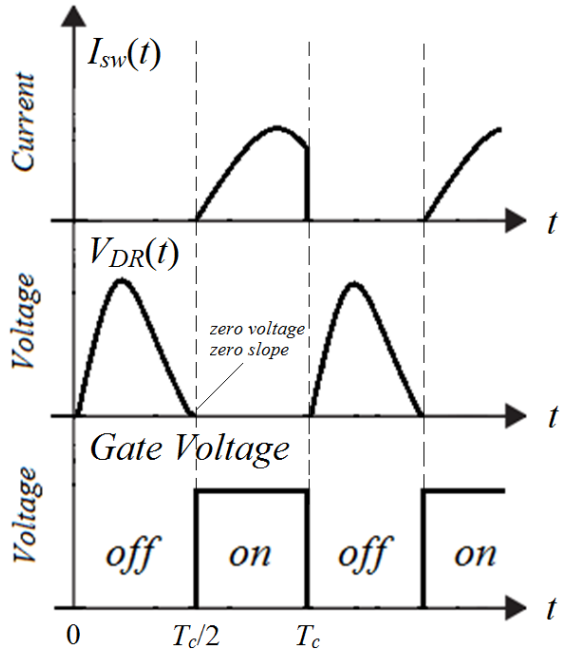

Figure 2.3. Conceptual waveforms of $I_{sw}(t)$ and $V_{DR}(t)$ under ZVS condition.

2.3 Class-E amplifier in a WPT system

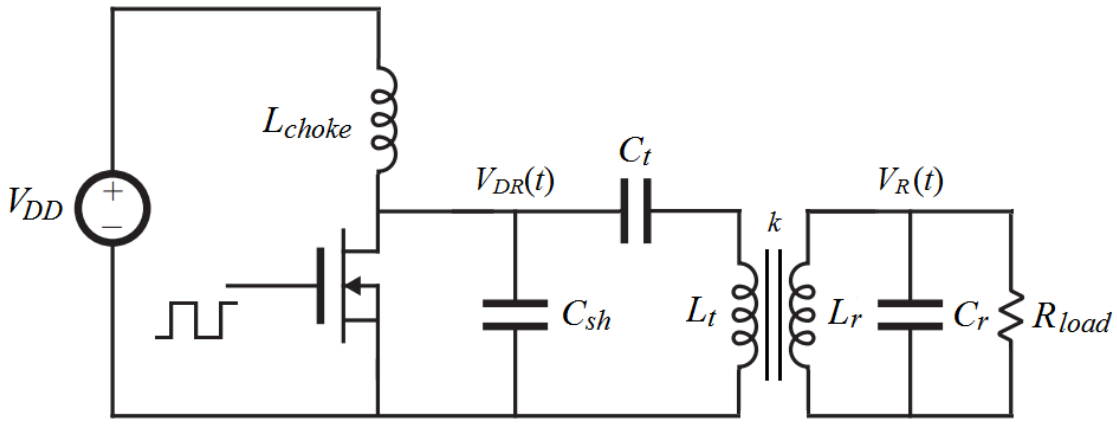

Figure 2.4. WPT system with class-E PA driver.

In Figure 2.4, we can see the class-E amplifier acting as the main driver for the WPT system. The load network simply comprises of a transmitter coil L_t mutually coupled with the receiver coil L_r which is tuned to resonate at the carrier frequency f_c with the parallel capacitor C_r. R_{load} will serve as the load of the system; it is the voltage across this element which we desire to regulate. Since our load isn't simply a resistor and an inductor but rather a primary coil L_t, mutually coupled with a parallel resonance circuit via the secondary coil L_r, we must design the class-E amplifier around the real and imaginary components of the total impedance $Z(j\omega_c)$ where ω_c is the frequency of operation of the class-E amplifier. This impedance can be conceptually seen in Figure 2.5.

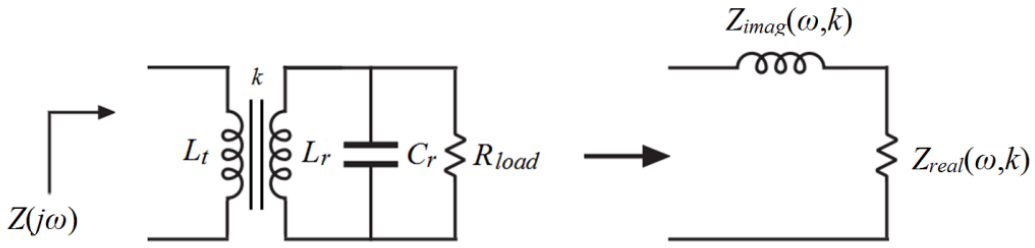

Figure 2.5. Total reflected load impedance $Z(j\omega)$ simply seen as an inductor and a resistor.

The total impedance is equivalent to,

$$Z(j\omega) = ((R_{load}||Z_{Cr} + Z_{mr})||Z_m) + Z_{mt} \tag{8}$$

where

$$Z_{Cr} = \frac{1}{j\omega C_r}, \tag{9}$$

$$Z_{mr} = j\omega(L_r - L_m), \tag{10}$$

$$Z_{mt} = j\omega(L_t - L_m), \tag{11}$$

$$L_m = k\sqrt{L_r L_t}, \tag{12}$$

and L_m being the mutual inductance between L_r and L_t where k is the coupling factor ranging from 0 to 1, with 1 being ideally coupled.

2.4 Coil misalignment

One major problem with wireless power transfer is the changes in the power delivery due coupling variations. In the case of wirelessly powered biomedical implants, the coils are most susceptible to misalignment because of muscle movements or misplacements.

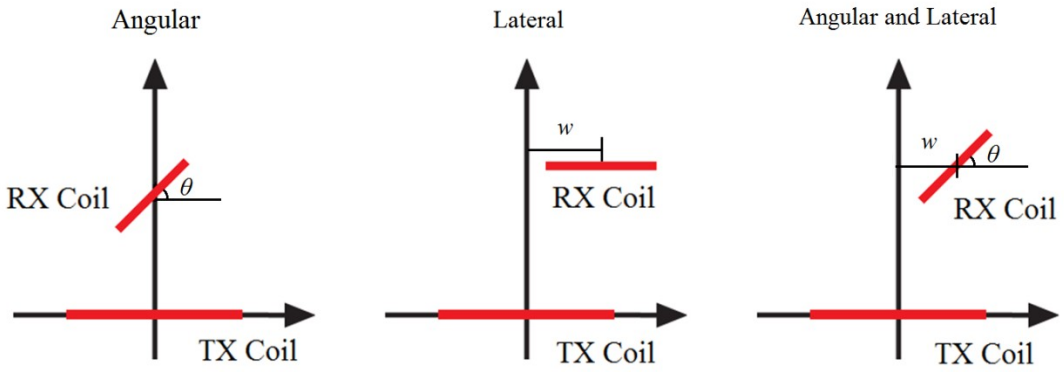

Figure 2.6. Coil misalignment can be angular, lateral, or both [8].

Changes in the coupling factor leads to changes in the load voltage [5] which can have detrimental effects. For example, if the coupling is too strong and too much power is being delivered to the secondary coil, the coil can start to heat up due to parasitic resistances. On the other hand, if the coupling is too weak, then not enough power can be delivered to sustain proper functionality of the implant [2]. So being able to tune and control the load voltage under coil misalignment is desirable. In terms of wireless power

transfer coils, this coupling coefficient is dependent on the geometrical placement of the two coils with respect to one another [8]. In Figure 2.6 it is shown that there are typically three forms of misalignment; angular, lateral or a combination of both. Angular misalignment occurs when both coils are centered along the vertical axis and one of them is tilted by an angle θ. Lateral misalignment occurs when both coils are parallel to each other, but their center locations are displaced laterally by a distance w. Since the impedance $Z(j\omega)$ is dependent on k, any changes in the coupling factor could cause $I_o(t)$ to change, which would thus cause the load peak voltage to change as described by the equation [5], that is

$$V_{rpeak} = I_o k \sqrt{L_r L_t}\,\omega \frac{|Z_{load}(j\omega)|}{|Z_{rec}(j\omega)|}\,, \tag{13}$$

$$|Z_{load}(j\omega)| = \frac{R_{load}}{\sqrt{1+(\omega R_{load} C_r)^2}}\,, \tag{14}$$

$$Z_{rec}(j\omega) = R_r + jIm_r, \tag{15}$$

$$R_r = \frac{R_{load}}{\sqrt{1+(\omega R_{load} C_r)}}, \tag{16}$$

$$Im_r = \frac{\omega\left(L_r - R_{load}{}^2 C_r\right)}{1+(\omega R_{load} C_r)^2}\,, \tag{17}$$

where $|Z_{load}(j\omega)|$ is the load impedance comprising of Z_{Cr} and R_{load}, and $|Z_{rec}(j\omega)|$ is the total impedance of the receiver [5]. But it is not only the load voltage regulation that is of concern, coupling also plays a role in the efficiency loss of the entire system. One important thing to consider is that since $Z(j\omega)$ changes with coupling, the ideal or optimal

operating condition of the Class-E amplifier will be thrown off balance. When this happens, the ZVS condition will not be met thus causing inefficient power dissipation in the FET and requiring the tuning of parameters to compensate for this misalignment. Research has been done to combat this problem of efficiency [3], [5], [9], [10], [11], [25], [26]. That being said, it is still in our best interest to have a technique that will deal with the efficiency and peak regulation simultaneously when designing a system. A wireless power transfer unit that regulates the load voltage but doesn't correct itself for efficiency undermines the use of a highly efficiently inverter such as the class-E amplifier. But again, since compensation for the class-E amplifier's efficiency is beyond the scope of this thesis, we will only deal with peak regulation.

2.5 Load voltage regulation work review

Several techniques have been proposed to combat load voltage regulation. Although efficiency loss is usually compensated through duty-cycle control, carrier frequency control and component tuning [3], [5], [9], [10], [11], [25], [26] the load voltage regulation is most easily achieved through the control of the power supply [2], [3], [4], [12], [22], [23]. Since the goal here is that the tuning be done automatically through feedback control, there has to be a way to measure a close estimate of the actual load peak voltage. In [4], a method is proposed where they measure the power level on the receiver side and send it to the transmitter side via amplitude-shift-keying (ASK) data communication through reverse telemetry using load modulation. After some further processing of this data signal, a binary signal is generated, representing the desired supply voltage value for compensation. This binary signal is then inputted to a power

control unit containing a DC/DC converter which supplies the corresponding supply voltage to the class-E amplifier. The system level diagram is shown in Figure 2.7. The work also provides feedback analysis in which the system is simplistically modelled as lumped elements and MATLAB/SPICE simulations are performed showing the response of the secondary side voltages under a 5mA load current change and with various coupling conditions.

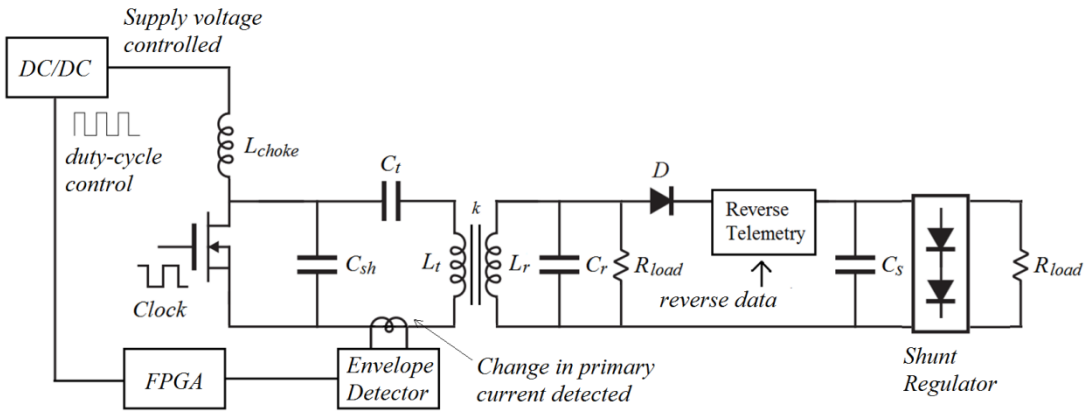

Figure 2.7. System level diagram of method proposed in [4].

The work in [23] describes a closed loop wireless power transfer system intended for stable power delivery to brain implants that involve multi-electrode arrays. Since overheating in the electronics from excessive power delivery can damage neurons and cause tissue damage, the power delivery must be controlled. In their design they utilize a class-E amplifier operating at 13.56 MHz to drive a primary coil which will wirelessly provide power the implant side via the secondary coil. The coils were fabricated on a PCB and their characteristics were simulated using the electromagnetics simulation software, Ansoft HFSS. The system uses time-division-multiple-access to communicate request information between the transmitter and the implant; this is done by load

impedance modulation and the information is transmitted along with same coils. The modulation of the load impedance is done from the secondary side in discrete pulses to induce a pulse-like change in the primary voltage. A single pulse means that power delivery needs to decrease and a double pulse means that power delivery needs to increase. This microcontroller takes in the pulse information via an ADC, and depending on whether it's two pulses or one pulse, it respectively increases or decreases the duty-cycle of the DC/DC power converter, which adjusts the supply voltage of the class-E amplifier. Figure 2.8 depicts the block diagram.

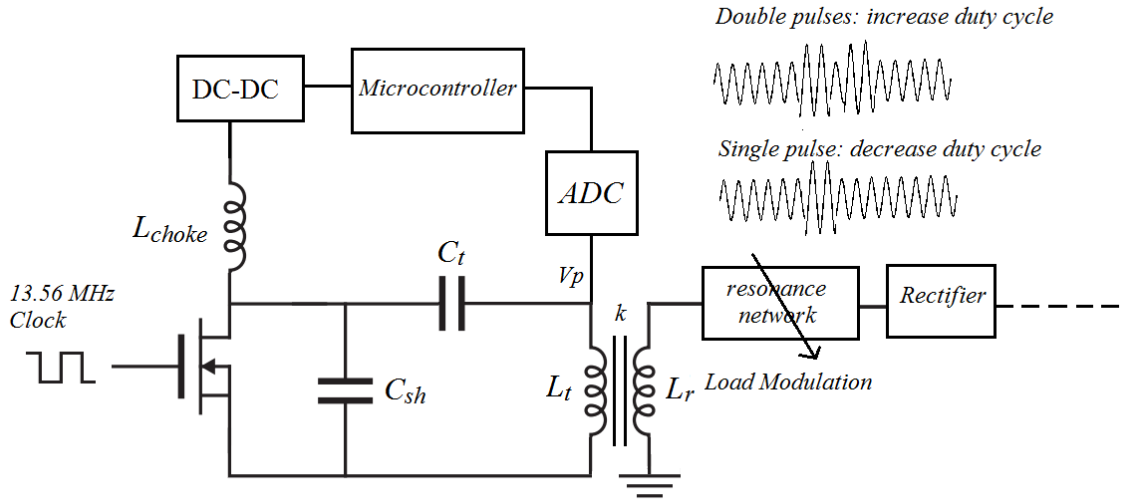

Figure 2.8. System block diagram of wireless power transfer system in [23].

In [12] a similar control topology is considered, except there is a software power control algorithm present in which the researchers make use of a 12-Bit USB-6008 from National Instruments for data logging. Similar to the previous example, the load voltage data is tapped off the secondary side through a peak detector circuit, along with the primary coil voltage and current. These measurements are sent through an ADC and into the USB-6008, from which it is sent into a computer running a power control algorithm on

MATLAB/Simulink. From the computer and into a DAC, a voltage signal is sent into a buck converter which decides the power supply voltage of the class-E amplifier. In their experiment, as the receiver coil's position moved from the left edge to the right edge of the primary coil in a span of 16 cm, the DC/DC converter generated output voltage from 9.4V to 11.3V to keep the receiver power at 2W constantly. System level design is shown in Figure 2.9.

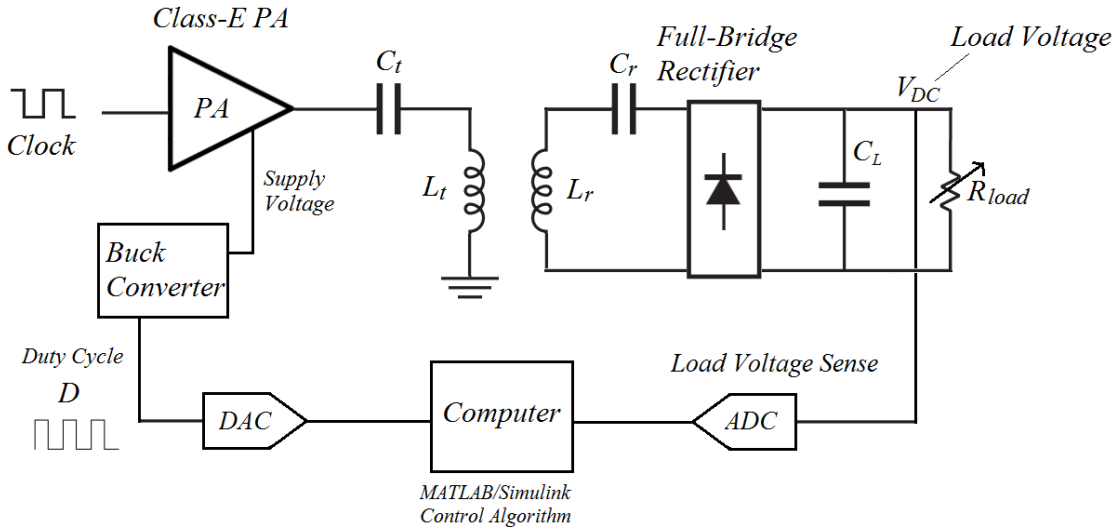

Figure 2.9. System level diagram of method proposed in [12].

In [3], the researchers present an architecture where power supply control is taking place as well as load compensation for efficiency loss. Based on the load resistance changes, the change in output power level is detected giving information about the class-E amplifier's operating condition and the actual voltage level across the load. For load voltage regulation, a power control loop adjusts the gate voltage of a pass transistor which controls the current flowing through the amplifier's inductor choke. Once the power efficiency is realizable and measured, a binary command signal is sent to a capacitor bank unit which then selects the proper capacitor to compensate for the loss in

efficiency. With compensation, they were able to achieve efficiency levels of around 81% across various loads, as opposed to an attenuating efficiency from 70% to 20% with no compensation. Figure 2.10 depicts their proposed control loop architecture.

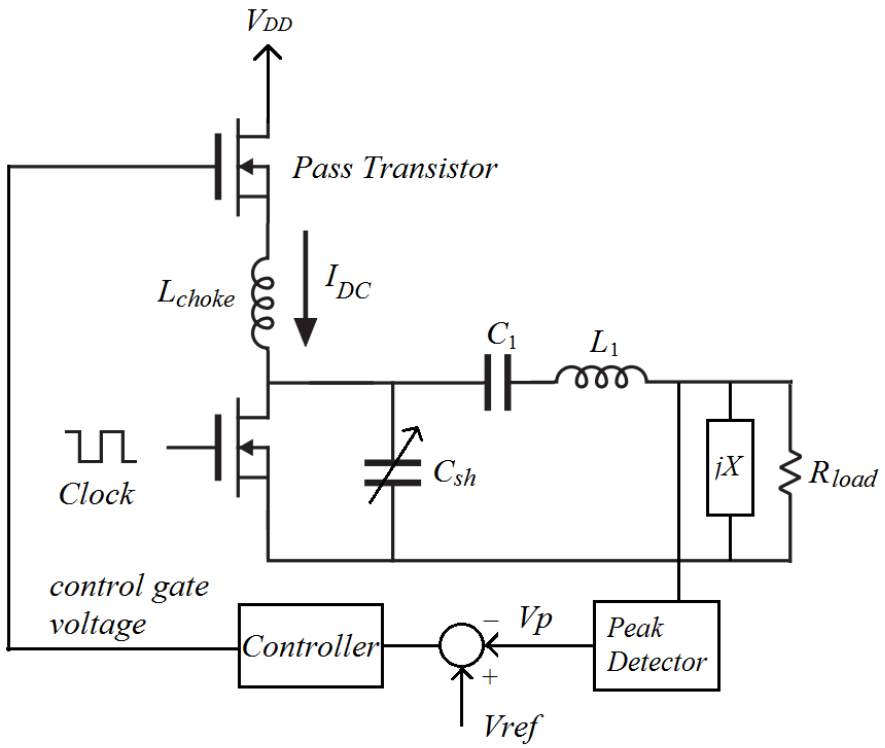

Figure 2.10. Power control loop of the proposed architecture in [3].

In [22], instead of a class-E amplifier, a push-pull resonant converter is used to drive the primary coil. The secondary coil is placed inside the body and receives the power. Then, using a full-bridge rectifier, AC power is converted to DC power with additional filtering via an LC network. The receiver side also contains a detection block where the output DC voltage level is converted into a digital signal through an ADC and after some processing, is transmitted to the transmitter side using RF communication transceivers. The transmitter contains a data processing unit that decodes this data and thus providing the output DC voltage level. This voltage level is then compared with a reference and a

control signal is sent to a variable DC/DC converter which adjusts the DC input of the push-pull resonant converter. With this feedback mechanism the output DC voltage is stabilized under coupling variations between the transmitter coil and receiver coil implanted in the body. Figure 2.11 illustrates the system level diagram of the architecture. Experimental data is presented showing the regulation of the output DC voltage to lateral misalignment between the coils.

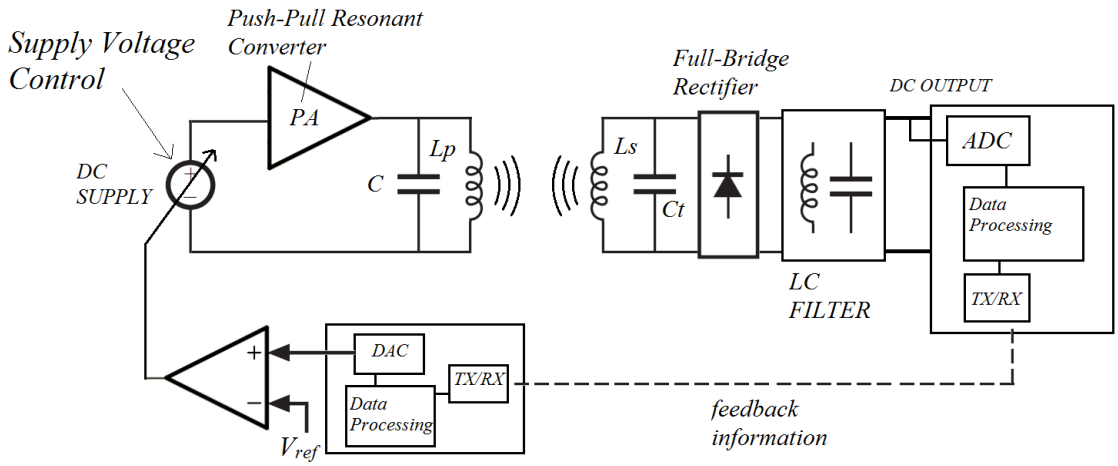

Figure 2.11. Transmitter utilizing a push-pull driver and power supply control [22].

So far, work has been presented where feedback has been performed with some form telemetry. In [20], it is presented that it is possible to in fact determine the output voltage with measuring state variable on the primary side. The benefit of this technique is that it removes the need of telemetry or any RF communication links that use power. The proposed method requires that all system parameters such as the coil inductances, mutual inductances, parasitic resistances, and resonant capacitances be known. Doing so allows the estimation of the load resistance and load power by simply measuring the transmitter coil's voltage and current. Frequency tuning control is performed in order to achieve

optimal efficiency. By using a look-up table, an operating frequency is selected corresponding to an estimated load impedance which would allow the system to work in optimal conditions; this solves for regulating efficiency. By estimating the output power level based the primary state variables, the input power can be adjusted in order regulate the output power. Although this technique is attractive, it requires that mutual inductance between the coils be known; and this of course is a much more difficult parameter to measure.

2.6 Conclusion

In this chapter, the class E amplifier and its role in the WPT system architecture was presented. Then the misalignment issue and its effect on the load voltage were introduced. The chapter ended with a literature review of misalignment compensation techniques for regulating the load voltage under coupling variations. In order to design a controller based on power supply control, a transfer function characterizing the open-loop behavior is needed. In the next chapter, a power supply control architecture is proposed to address the load voltage regulation problem while taking into account the open-loop transfer function in its controller design.

Chapter 3

Proposed Load Voltage Regulation Method

As discussed in Chapter 2, power supply control technique is a desirable method for controlling the load voltage under coupling changes. If changes in the coupling coefficient cause changes to the load voltage, the supply voltage can be tuned to compensate for this change accordingly.

In this chapter a feedback control architecture is proposed for load voltage regulation problem. Because a feedback controller cannot be designed without knowing the transfer function of the open-loop system, the transfer function of the open-loop system is first analytically derived. Once the open-loop transfer function is obtained, the design of the controller is discussed. Although efficiency concerns are beyond the scope of this thesis, a brief discussion is made regarding the regulation's effect on the efficiency of the boost converter.

3.1 The open-loop system

In order to change the initial value of the DC supply voltage to a new voltage value, a switch-mode DC-DC converter would work best. Switching regulators have an advantage over the linear regulators in efficiency performance; although linear regulators are less noisy since they are DC coupled [13]. The most suitable switching topologies for this application would be buck converters and boost converters. In the proposed method, a

boost converter will be used. The output of the boost converter is connected to the supply end of the class-E amplifier, as shown in Figure 3.1.

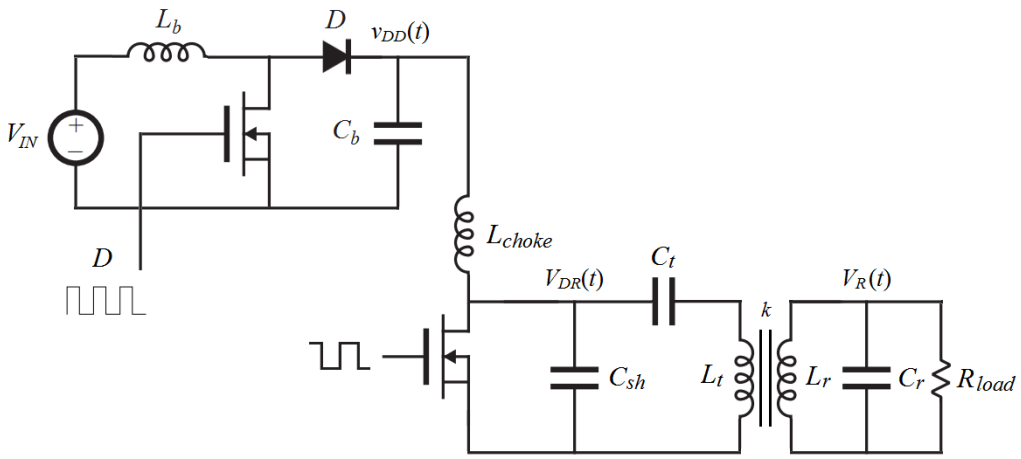

Figure 3.1. Boost converter is used to control the class-E PA's supply rail.

By varying the boost converter's PWM signal's duty-cycle D, the supply voltage V_{DD} can be tuned as according to (18),

$$V_{DD} = V_{IN}\left(\frac{1}{1-D}\right) \tag{18}$$

This equation assumes 100% efficiency and that the components of the boost converter are ideal (i.e they don't contain any parasitic resistances). Figure 3.2 shows conceptually how variations in D, leads to variations in V_{DD}, which ultimately leads to variations in $V_R(t)$. One important thing to keep in mind is that we desire to control the amplitude or the peak of the load voltage. Therefore, knowledge of the instantaneous voltage is unnecessary because the load voltage is to eventually be rectified and filtered, leaving only a DC voltage supply for the implant.

The operation described above is for the system functioning in an open-loop configuration. Given we know our desired and measured load voltage amplitudes, and that our plant model is controllable through adjusting the duty-cycle, we now have our control problem.

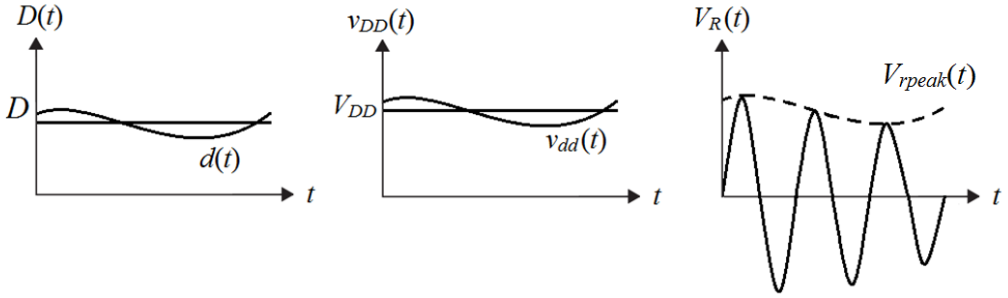

Figure 3.2. Idealized waveforms characterizing peak/envelope control.

3.2 Load voltage regulation via linear feedback control

Switch-mode power converters are commonly called switching regulators because they utilize feedback control to stabilize their output voltage. The control architectures commonly used are voltage-mode control and current-mode control, with the latter being the most popular. If we take a boost converter for example, the output voltage under loading generally droops depending on the time constant between the output capacitor and the load. In order to stabilize or regulate this output voltage at a desired reference, a error signal is first generated via comparing the actual voltage to this desired voltage. The error signal is then fed into a controller or linear compensator to which it becomes a control signal corresponding to a particular duty-cycle. For example, if the error is positive (i.e the output voltage is less than the reference), the higher duty-cycle from the pulkse width modulated control signal results in increasing the output voltage, and thus

we have feedback. The system-level diagram of this opertion typically known as voltage-mode control, is shown in Figure 3.3.

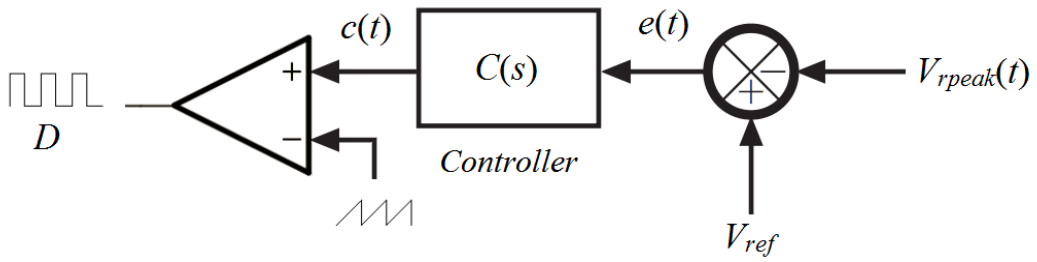

Figure 3.3. Basic architecture of PWM voltage-mode control.

Pulse-width-modulation (PWM) is achieved using a comparator where inverting input is fed with a ramp or sawtooth voltage, and the non-inverting is fed with the control signal $c(t)$. The duty-cycle of the PWM signal is linearly related to the amplitude of the control signal. If we were to cascade the WPT system to the end of the boost converter, we would get our original power supply control architecture. Just like how we did with the boost converter alone, it is possible to regulate the load peak voltage of the WPT system using voltage mode control. If the coupling between the links decreases, the decrease in load peak voltage corresponds to a positive error signal, thus increasing the boost converter's PWM signal's duty-cycle which would then increase the supply voltage. Using this simple voltage-mode control, load peak regulation is possible. Figure 3.4 depicts the full closed loop architecture.

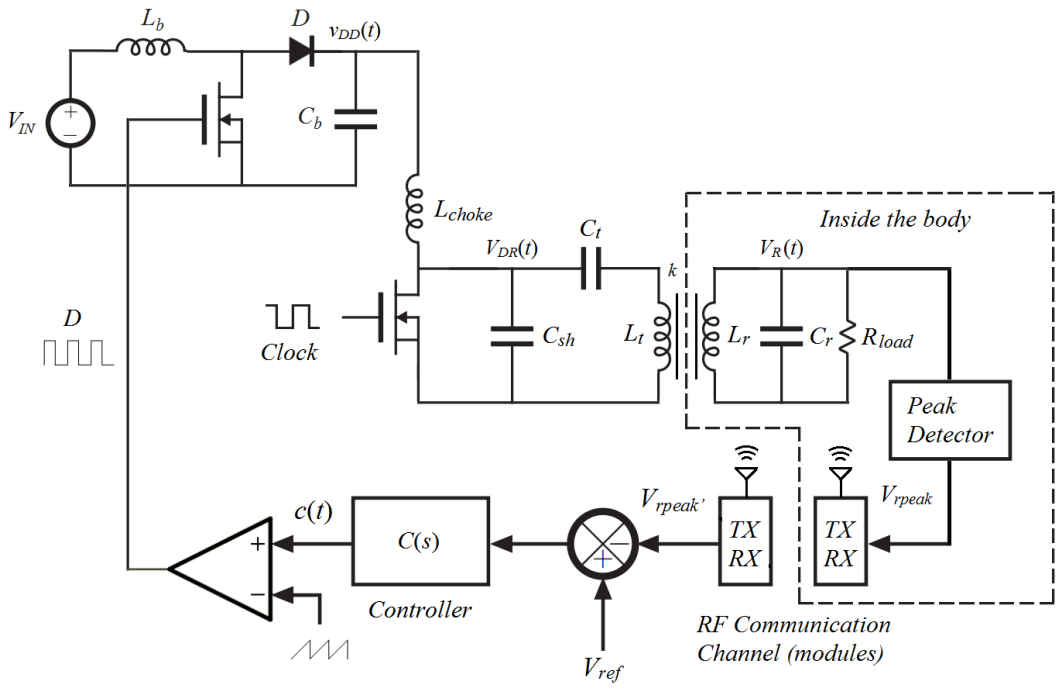

Figure 3.4. WPT system utilizing voltage-mode control.

This is a very general and system-level design of the control system since it doesn't take into consideration the transportation delay or time lags associated with carrying the feedback information from the receiver side to the transmitter side. For system-level modeling purposes, the propagation from capturing the envelope load voltage $V_{rpeak}(t)$ from the receiver side to transmitting it to the transmitter side as a feedback signal is portrayed in Figure 3.5.

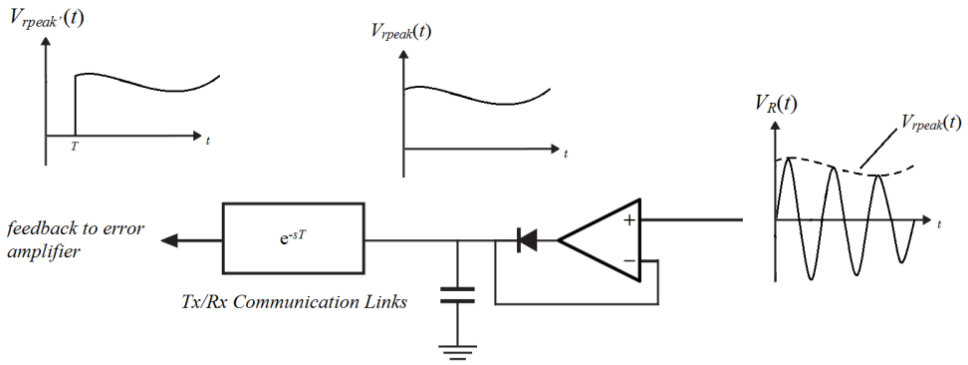

Figure 3.5. Modeling the feedback sensing transport delay.

There will be some time delay T between sending the information from the receiver to the transmitter using some form of communication protocol. So the time delay can be modeled in its Laplace form as e^{-sT} where T is the time delay [2]. This property is important for controller design, but for the sake of simplicity it will ignored in the transmission loop. The peak detector's op amp in Figure 3.5 is assumed to be supplied by the rectified and filtered DC voltage. Assuming a full-bridge rectifier is used, and that each diode contributes a 0.7V voltage drop, the supply rail of the peak detector's op amp will be equal to V_{rpeak} – 1.4V because the full-bridge rectifier contributes two diode voltage drops. The problem with this is that the input is now larger than the supply rail voltage. In order to fix this issue, a high impedance voltage divider network can be used to sample a lower voltage into the non-inverting input of the op amp. This way, the non-inverting input voltage can be set so that it is always lower than the supply rail voltage.

Another problem is how the variation in delivered power can impact the performance of the op amp. In addition, before designing the receiver-side sensing circuitry (including the RF communication link), the designer must know the power delivered to the receiver-side under the worst-case scenario. This worst-case scenario translates to the weakest acceptable mutual coupling for a given WPT application.

Now that we have the power supply control architecture in place, the compensator must be designed in accordance to the gain and phase information of the open-loop system relating the duty-cycle variation $d(s)$ to the load peak voltage variation $V_{rpeak}(s)$. In the next section, we will try to obtain an approximate transfer function relating $d(s)$ to $V_{rpeak}(s)$.

3.3 Obtaining the open-loop transfer function

For the controller design, a controller or compensator cannot be designed without obtaining the gain and phase information of the plant model. We can see that the input of our plant is the PWM signal into the gate of our boost converter, and the output is the envelope of the load voltage on the secondary end. In this section we will try to come up with an appropriate transfer function that models the variations in the duty cycle of the PWM control signal with respect to the AC variation of the envelope of the load voltage, as depicted in Figure 3.6.

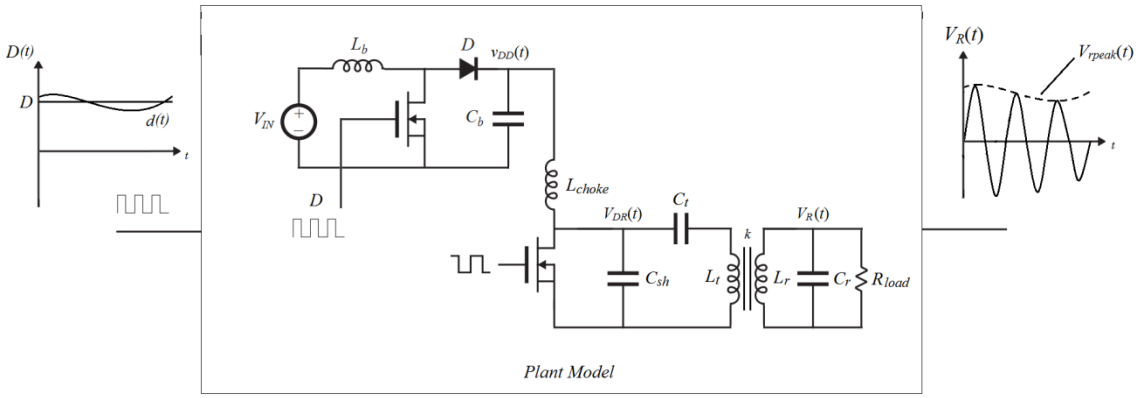

Figure 3.6. Open-loop system or plant with the input $d(t)$ and output $V_{rpeak}(t)$.

The first step is to find the transfer function that relates the AC variation of the control input (i.e. the duty cycle) of the boost converter to the envelope of $V_{DR}(t)$ or the voltage at the drain of the class-E amplifier's FET. We first look at deriving the small-signal model of the boost converter. For a given or desired input and output DC voltage, and a duty cycle, any AC variation in the duty cycle $d(s)$ should induce an AC variation in the boost converter's output voltage $v_{dd}(s)$, and the magnitude and phase relation between these two variables is described through a model, usually noted as the control-to-output transfer

function $G_{vd}(s)$. Since this system is non-linear due to the switching behavior, an averaging or linearization technique is used where all the switching harmonics in the states are removed by averaging the waveforms over a switching period or interval T_{sw}. This linearizes the system, and it's now possible treat it as a linear time invariant system. The derivations of the transfer function of switch-mode converters using this technique are described more analytically in [14]. The transfer function of the boost converter is obtained as (a two pole system),

$$G_{vd}(s) = G_{d0}\frac{1 - \frac{s}{\omega_z}}{1 + \frac{s}{Q\omega_0} + \left(\frac{s}{\omega_0}\right)^2}, \tag{19}$$

where,

$$G_{d0} = \frac{V_o}{1 - D}, \tag{20}$$

$$\omega_0 = \frac{1 - D}{\sqrt{L_b C_b}}, \tag{21}$$

$$Q = (1 - D)R\sqrt{C_b / L_b}, \tag{22}$$

and the right-hand zero located at,

$$\omega_z = \frac{(1 - D)^2 R}{L_b}. \tag{23}$$

But in this model, the assumption is that the output of the boost converter is purely resistive. Since we're loading the boost converter with the supply end of the class-E amplifier, we will have a complex impedance looking into the load. Looking into the

supply end of the class-E amplifier, the load to the boost converter can be simplistically modeled with a series combination of the RF choke inductance L_{choke} and a DC resistance $R_{dc} \approx V_{DD}/I_{DD}$. For a class-E amplifier operating under optimal conditions, $R_{dc} \approx 1.733 Z_{real}(\omega,k)$ [7]. This forms a single pole low-pass filter in the modulation path [7]. Figure 3.7 shows the boost converter with the complex load. Since R_{dc} is the effective resistance across the class-E amplifier's MOS drain, its DC voltage can be represented as the average of the drain voltage $V_{DR}(t)$ [15].

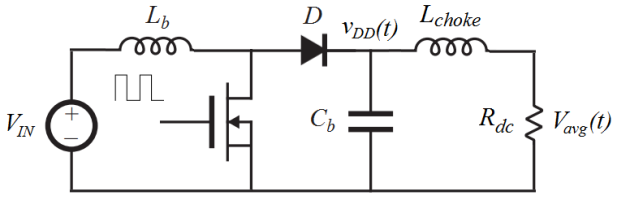

Figure 3.7. Boost converter with a complex load (L_{choke} and R_{dc}).

The average of the drain voltage $V_{avg}(t)$ is expressed in (24) and conceptually shown in Figure 3.8.

$$V_{avg}(t) = \frac{1}{T_c}\int_{t\text{-}T_c}^{t} V_{DR}(t)\,dt\,. \tag{24}$$

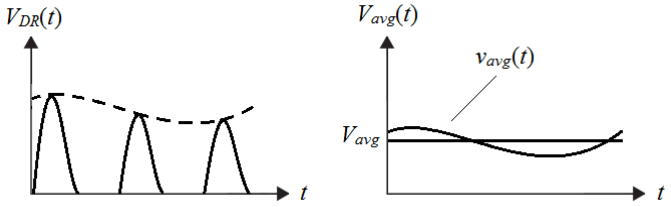

Figure 3.8. $V_{avg}(t)$ is the effective voltage across R_{dc}.

So the load of the boost converter is effectively a series combination of L_{choke} and R_{dc}. Using the same linearization technique used in [14], [16] derives a small-signal model of a

boost converter but with a complex load impedance conveniently consisting of a resistor and an inductor. The control-to-output transfer function is obtained as

$$P(s) = \frac{v_{dd}(s)}{d(s)} = -P_0 \frac{(s - \omega_{zp})}{(s+\omega_1)(s^2+2\xi\omega_0 s+\omega_0^2)}, \tag{25}$$

where, neglecting parasitic such as the DCRs in L_b and L_{choke}, and the ESR in C_b

$$\omega_1 = \frac{R_{dc}}{L_{choke}}, \tag{26}$$

$$\omega_0 = \sqrt{\frac{(1-D)^2}{L_b C_b}}, \tag{27}$$

$$\xi = \frac{L_b}{\sqrt{L_b C_b R_{dc}^2 (1\text{-}D)^2}}, \tag{28}$$

and a zero presented at

$$\omega_{zp} = \frac{R_{dc}(1-D)^2}{L_b - (1-D)^2 L_{choke}}. \tag{29}$$

Lastly the low-frequency gain is found as

$$P_0 = \frac{\omega_0^2 \omega_1 V_O}{\omega_{zp}(1-D)}. \tag{30}$$

It is evident from (25) that the boost converter with the complex load contributes three poles, and one zero. This transfer function $P(s)$ only relates $d(s)$ to $V_{dd}(s)$; what is of interest is the small-signal component across R_{dc} or $v_{avg}(s)$. This is easily obtained by

$$\widehat{P}(s) = P(s) \frac{1}{\frac{s}{\omega_1} + 1}, \tag{31}$$

where $\widehat{P}(s) = v_{avg}(s)/d(s)$.

Now that we've reached this far in our modulation path, lastly, a function relating $v_{avg}(s)$ to the load peak voltage $V_{rpeak}(s)$ is needed. Taking a very rough approximation, since the class-E amplifier performs reasonably well as a linear amplitude modulator [10], the transmission between $v_{avg}(t)$ to $V_{rpeak}(t)$ can be seen simply as a gain. This gain can be obtained by first finding the function relating the fundamental component of the drain voltage to the voltage across the real component of the reflected impedance looking into the primary coil L_t [5]; the real and imaginary components will be denoted as $Z_{real}(\omega,k)$ and $Z_{imag}(\omega,k)$ respectively and the modulating amplitude across $Z_{real}(\omega,k)$ as $V_t(t)$. $X_{imag}(\omega,k)$ is equal to $Z_{imag}(\omega,k)/\omega$ and represents the reflected inductance value. Since this reflected impedance is in series with C_t, it forms a series-tuned *R-L-C* network which has a 2nd-order transfer function $K_c(j\omega)$; Figure 3.9 depicts the WPT system where the load network is roughly approximated.

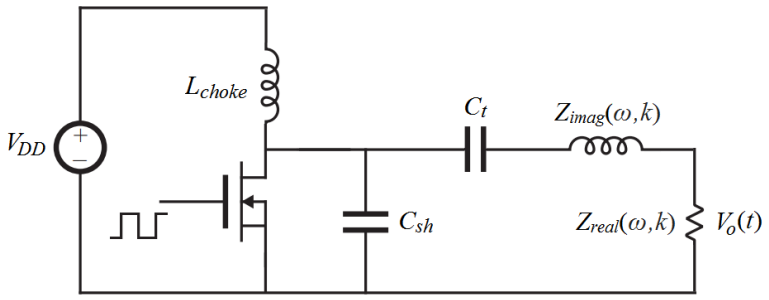

Figure 3.9. Load network seen as equivalent impedance comprised of $Z_{real}(\omega,k)$ and $Z_{imag}(\omega,k)$.

The design equations of the class-E amplifier must be designed around this load network. In Chapter 2 it was discussed that an extra inductance is added in series to introduce a current lag to fulfill the ZVS condition. This extra inductance is absorbed into $X_{imag}(\omega,k)$, so only a part of $X_{imag}(\omega,k)$ is precisely resonance-tuned with C_t at the frequency f_c.

From this transfer function $K_c(j\omega)$, the gain or magnitude from the drain to $Z_{real}(\omega,k)$ at ω_c is [7],

$$\left|K_c(j\omega_c)\right| = \frac{Z_{real}}{X_{imag}}\left|\frac{j\omega_c}{(j\omega_c)^2 + \frac{Z_{real}}{X_{imag}}j\omega_c + \frac{1}{C_t X_{imag}}}\right| . \tag{32}$$

The equation relating the current amplitude through $Z_{real}(\omega_c,k)$ to the voltage amplitude across R_{load} is described in (13). Since we want to relate the voltage amplitude across to $Z_{real}(\omega_c,k)$ to the voltage amplitude across R_{load}, we can arrange the equation as

$$V_{rpeak}(t) = V_t(t)\left(k\omega_c\sqrt{L_r L_t}\frac{|Z_{load}(j\omega_c)|}{Z_{real}(\omega_c,k)\left|Z_{rec}(j\omega_c)\right|}\right), \tag{33}$$

where $V_t(t)$ is the modulating amplitude of $V_o(t)$, and $V_{rpeak}(t)$ is the modulating amplitude of $V_R(t)$. $Z_{load}(j\omega_c)$ represents the load impedance at the receiver, and $Z_{rec}(j\omega_c)$ as the receiver's total impedance. Multiplying out (32) and (33), we can simply approximate that the relation between $v_{dd}(s)$ to $V_{rpeak}(s)$ as a gain K_o

$$K_o = \left|K_c(j\omega_c)\right|\left(k\omega_c\sqrt{L_r L_t}\frac{\left|Z_{load}(j\omega_c)\right|}{Z_{real}(\omega_c,k)\left|Z_{rec}(j\omega_c)\right|}\right) . \tag{34}$$

Taking the single-pole filter into account and combining the transfer functions, we get that the open loop system is approximately

$$A_o(s) = \frac{V_{rpeak}(s)}{d(s)} \approx K_o\widehat{P}(s) . \tag{35}$$

Now that we have obtained the transfer function relating $d(s)$ to $V_{rpeak}(s)$, we can now move onto the design of the controller, which will be discussed in the next section. One

disclaimer to note is that this transfer function is dependent on the biasing of the system; as k and D change, the entire transfer function changes. In addition, due to coupling variations, R_{dc} changes as well. So this controller should be designed for a bounded variation in coupling; if the coupling is drastically off from the bias, the controller may not keep up with the phase lags introduced by this new open-loop transfer function, thus risking instability or oscillation.

3.4 Linear controller design

Now that we have a good model characterizing our open-loop envelope control, we can move on to addressing the controller design. To avoid oscillations or instability, the controller or compensator must be designed such that the transmission loop function $T(s)$ meets the simple phase margin criterion [17]. Assuming there is no significant time delay in the data transmission between the communication links, we can model the control system block diagram as shown in Figure 3.10, where $C(s)$ is our controller. The measured envelope is compared with a desired reference to generate an error signal $e(s)$. This error signal is then fed into the controller to generate a small-signal control signal $d(s)$ which is to be coupled with a nominal bias duty cycle to form our PWM signal for the boost converter. The feedback works as such; if the peak envelope voltage increases slightly due to a coupling change, this measured envelope will be compare to the desired reference and generate a negative error, which corresponds to a negative control signal.

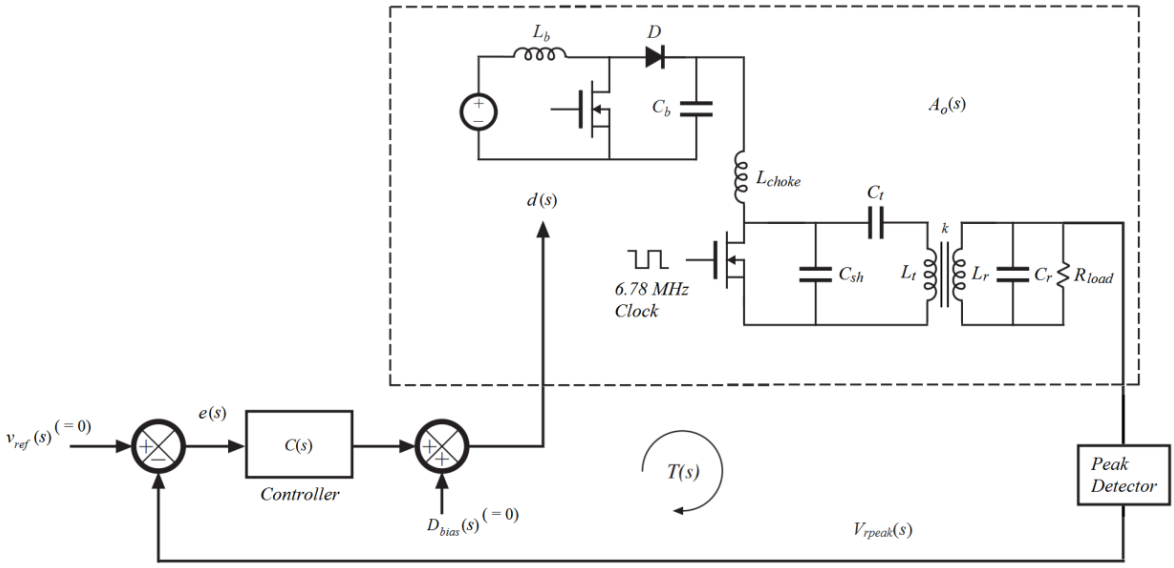

Figure 3.10. Closed-loop diagram for small-signal analysis and controller design.

This negative control signal summed with the bias duty cycle will drive the PWM signal to a smaller duty cycle which lowers the supply voltage and thus lowers the peak envelope voltage. This works vice versa for decreases in peak envelope voltage. The $v_{ref}(s)$ and $D_{bias}(s)$ are the small signal components of our desired reference peak envelope voltage and nominal duty cycle, respectively. Hence, their values must be zero since they only consist of their DC terms and take no part in the controller design. Also, intuitively it should be evident that since we want no variations in the envelope output, our desired envelope must be a constant DC component. Our transmission loop function $T(s)$ is now equal to

$$T(s) = C(s)\, A_o(s). \tag{36}$$

Where our closed loop transfer function is

$$A_{cl}(s) = \frac{T(s)}{1+T(s)}\ . \tag{37}$$

And in order to meet the stability criterion, the loop gain $|T(s)|$ must be lower than 0 dB at $\angle T(s) = 180°$ for the system to be stable and exhibit no oscillations or positive feedback. So depending of the open loop plant $A_o(s)$, the controller must be designed accordingly to meet the stability criterion.

Analytically designing $C(s)$ through techniques such as pole-placement or root-locus can be cumbersome by hand. Luckily MATLAB's Control Systems Toolbox contains a very useful PID tuning GUI, where by providing the open-loop transfer function or (35), the designer is given the K_p, K_i, and K_d values in respect to a desired closed-loop step response.

3.5 Effect on efficiency

Although this regulation technique does nothing to compensate for the efficiency loss in the class-E amplifier, it still plays a role in the efficiency of the entire system. If the coupling deviates far from the nominal coupling, more control action is needed by the boost converter. For example, if a large change in coupling causes the load voltage to drop drastically, the duty cycle will be driven to a higher value leading to more conduction loss in the boost converter's MOSFET. The MOSFET conduction loss contributes the largest component loss in switch-mode power converters and can be described approximately as

$$P_{con} = I_{avg}^2 R_{DS(ON)} D, \tag{38}$$

where I_{avg} is the average MOSFET current and $R_{DS(ON)}$ is the intrinsic drain-source ON resistance [21]. So the battery source must be chosen wisely so that high duty-cycles value

isn’t generated; the system should be biased properly such that only a little control action is required.

3.6 Conclusion

In order to design a controller for the WPT system an open loop model must be obtained. In this chapter, we derived the open-loop transfer function, which can be used to design the controller. In the Chapter 4, we will present the simulation results for both the open-loop and closed-loop system to validate the theoretical derivations and the efficiency of the proposed technique in load voltage regulation under misalignment.

Chapter 4

Simulation Model and Data

In Chapter 3 the proposed architecture and its operation was discussed and a transfer function was derived. Now that the theory is in place, in this chapter, a Simulink model is presented along with simulation results to evaluate the regulation in action. A comparison between the theoretical derived transfer function and a simulated transfer function for the open loop system is also shown in order to validate that theoretical derivation closely models the transfer function of the open-loop system. The response of the controller to variations in the coupling coefficient is also investigated.

4.1 Simulink model

After obtaining the open-loop transfer function $A_o(s)$ we must first verify that it's an approximate model through simulation. An ideal model was built in MATLAB's Simulink using the Power System Toolbox, which gives access to components such as MOSFETs, ideal diodes, and passive components. The component values chosen for the class-E amplifier were based off of design equations from [7] and are shown in the table 4.1 along with the chosen boost converter component values. The system was designed at a carrier frequency of 6.78 MHz in the ISM band, typically allocated for medical applications, among many other applications [18].

Table 4.1
Parameters of The Boost Converter

Parameter	Value
Operating Frequency f_{sw}	500 kHz
Bias Duty Cycle D	0.5
Input Voltage V_{in}	1.5V
Output Voltage V_{DD}	3V
Inductance L_b	2.7µH
Output Capacitance C_b	60µF
MOSFET's $R_{DS(ON)}$	0.05 Ω

Table 4.2
Parameters of The WPT System

Parameter	Value	
Operating Frequency f_c	6.78 MHz	
Bias coupling coefficient k	0.2	
Shunt Capacitance C_{sh}	3.66nF	
Primary/Secondary Capacitance (C_t/C_r)	91pF	51.4pF
Primary/Secondary Coil Inductance (L_t/L_r)	6.3µH	10.7µH
Load Resistance R_{load}	50 Ω	
Choke Inductance L_{choke}	25µH	
MOSFET's $R_{DS(ON)}$	0.54 Ω	

In Figure 4.1, the Simulink model of the open-loop system is shown. The boost converter's duty cycle is biased at 50% and the mutual coupling coefficient at $k = 0.2$. In order to validate (35) in Simulink, a sine-wave signal representing $d(t)$, was superimposed with the bias duty-cycle of 0.5 at an amplitude of 0.01. Manually varying the frequency of $d(t)$ from 400 Hz to 20200 Hz, the output load peak $v_{rpeak}(t)$ was measured in terms of its amplitude and phase shift using measurement cursors. This method is typically noted as the signal injection technique [19] and is an acceptable method for determining the open-loop transfer function.

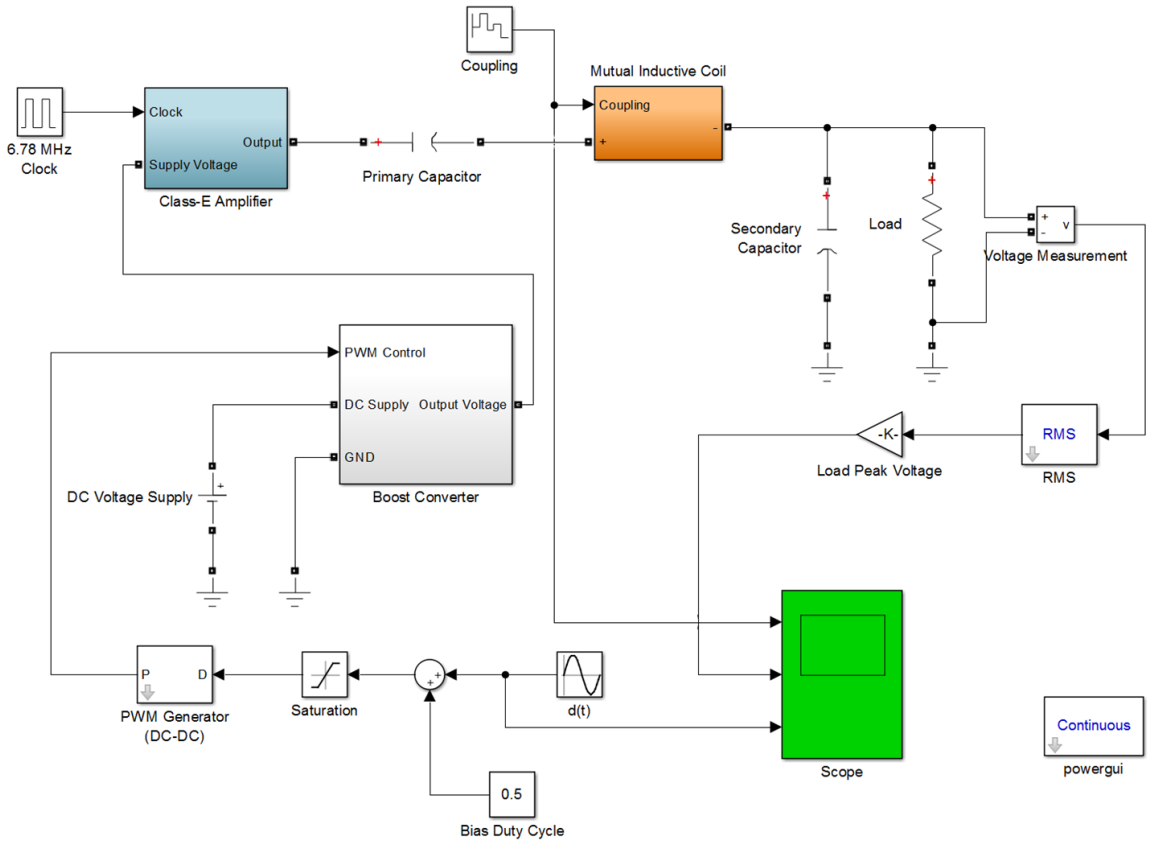

Figure 4.1. Simulink model of the open-loop system with variable mutual coupling.

Because none of the Simulink toolboxes contain a peak detector block, a RMS value block was used and then cascaded with a gain of 1.4141 to obtain the load peak value. A

saturation block is added between the PWM generator block to limit the control range to $0 < D < 0.9$. Using the signal injection method, the simulated bode plot was obtained and compared to (35)'s bode plot as shown in Figure 4.2. As can be seen from Figure 4.2, (35) closely models the dynamics of the open-loop system, and is sufficient enough for controller design despite the minimal error between the simulated and theoretical data.

Observing the system's open-loop behavior to coupling disturbances, we can see how the load peak voltage varies, (see Figure 4.3). The coupling disturbance is introduced using a stair-case block given the array [0.2, 0.22, 0.195, 0.205]. We can see that the load peak is deviating from the desired voltage of 12V which occurs when the coupling remains biased at 0.2. Clearly, we need feedback to regulate load peak voltage to a desired value.

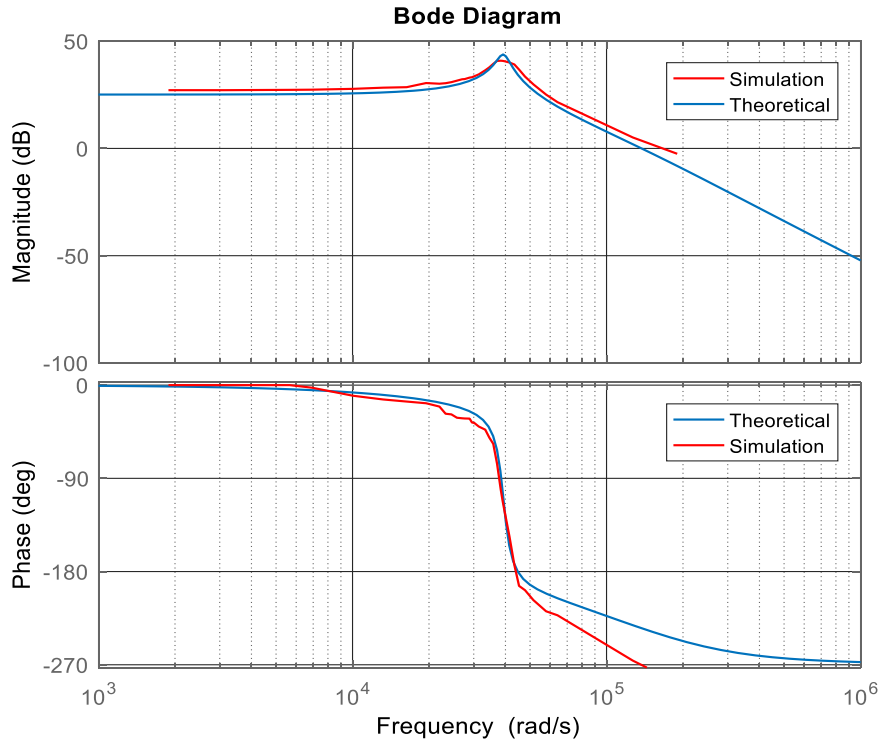

Figure 4.2. Comparison between the Bode plot of $A_o(s)$ and the simulated Bode plot.

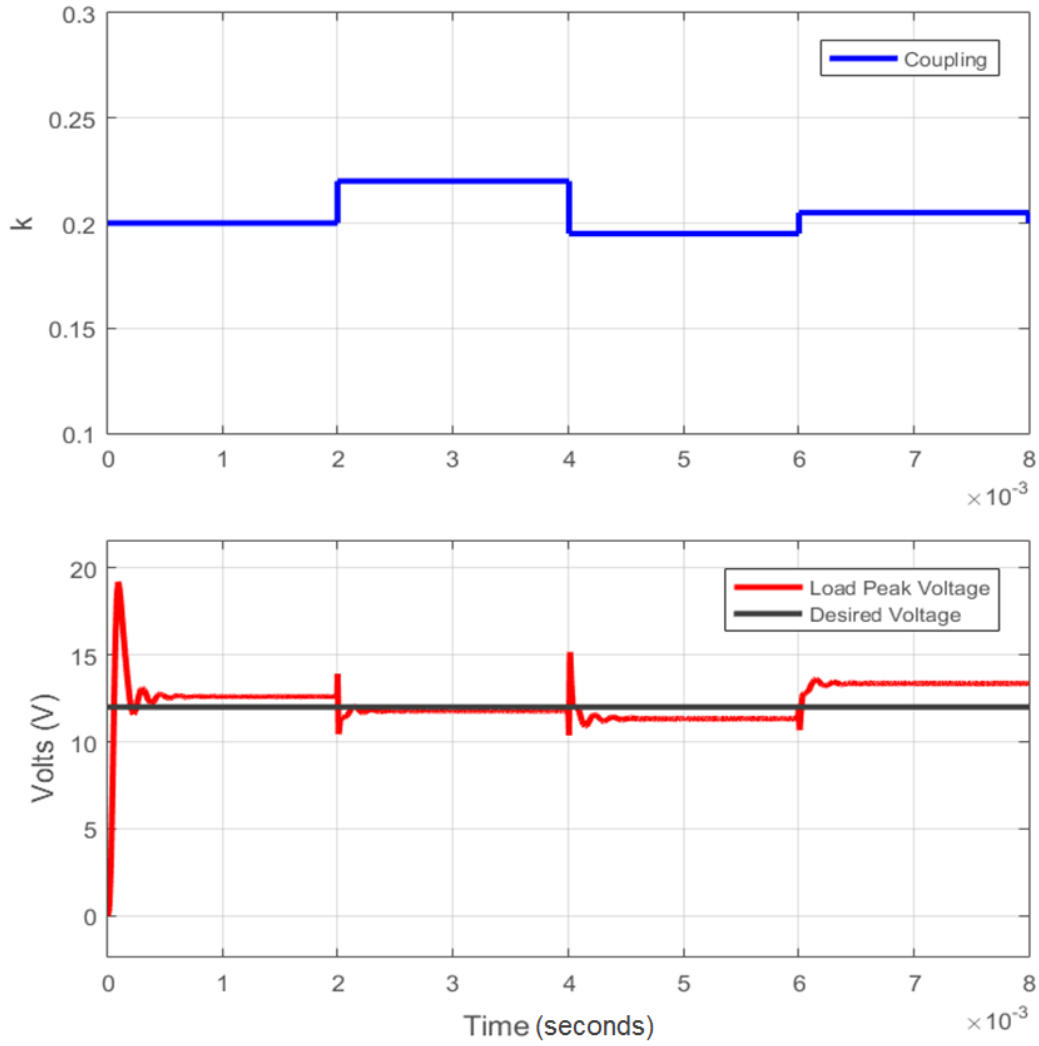

Figure 4.3. Peak load voltage unregulated under coupling variations.

Using (35) for the open loop transfer function and the PID tuning GUI, the integral controller's gain was chosen to be K_i = 82. An integral controller was added to the Simulink model to demonstrate the load peak regulation under step coupling variations. The closed-loop model can be seen below in Figure 4.4.

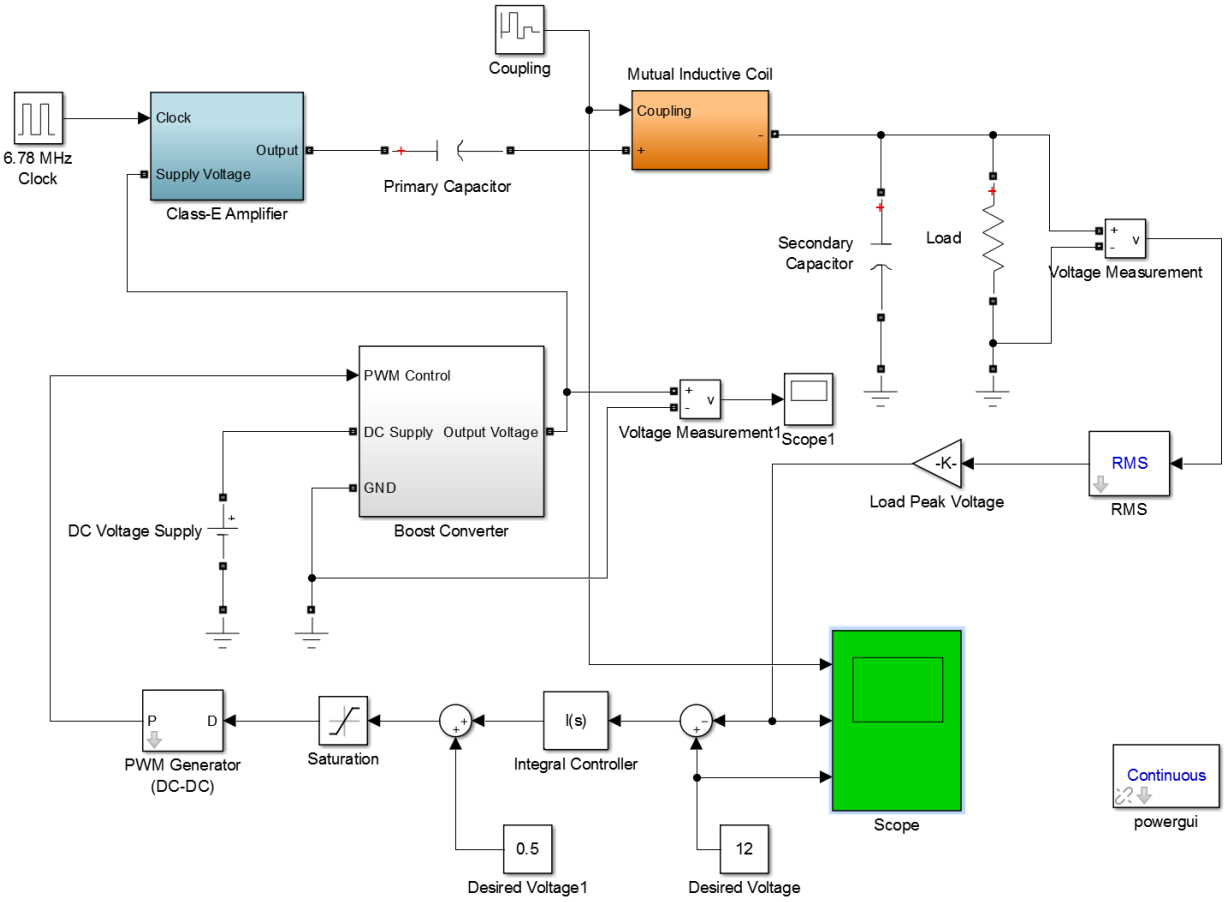

Figure 4.4. Simulink model of the closed-loop system utilizing an integral controller.

Figure 4.5 shows simulation results of the closed-loop model in action where the peak reference is set to 12V. We can see that the integral controller is doing a good job in regulating the load peak voltage under coil coupling changes. The coupling variations are in the form of step disturbances at 2 ms intervals and varying around a nominal value of $k = 0.2$.

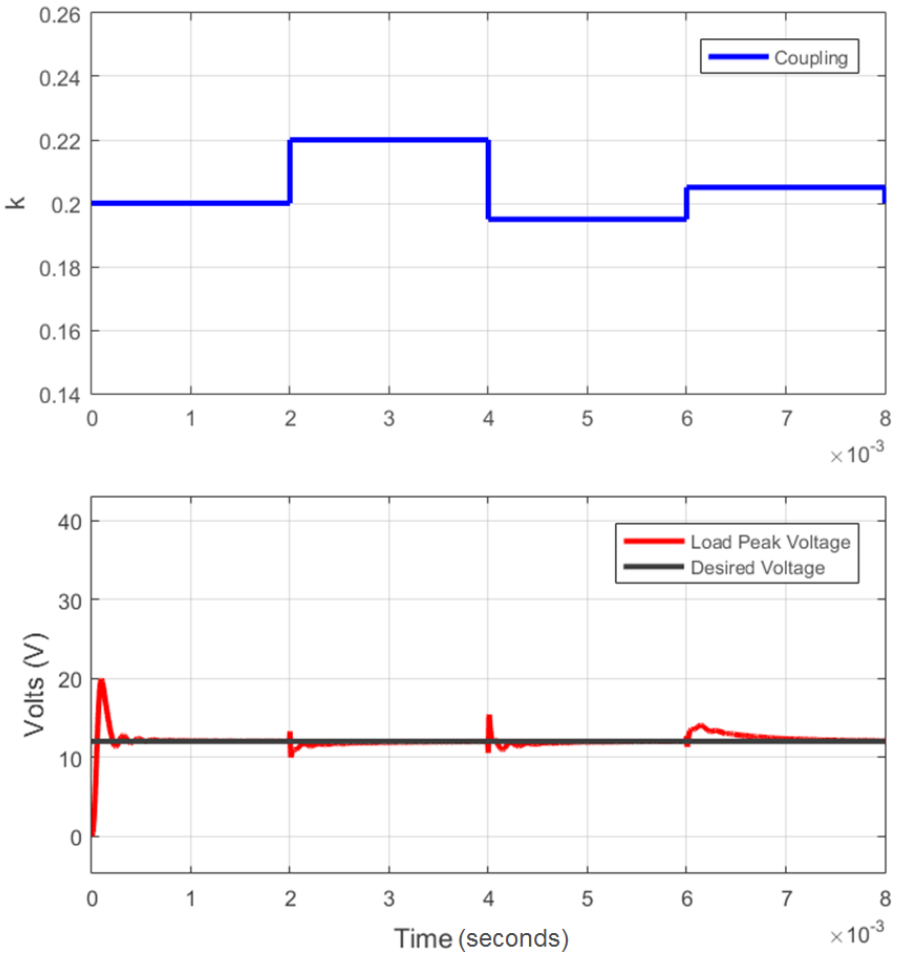

Figure 4.5. Peak load voltage regulation under coupling variations.

4.2 Discussions

The class-E amplifier was designed at a nominal coupling coefficient of 0.2, that being said, the optimal efficiency conditions will be thrown off once this coupling varies. So although power supply control will regulate the load peak voltage, other tuning techniques need to be incorporated as well to compensate for the efficiency loss [3], [5], [9], [10], [11]. One thing to note is that if there is a large change in the *k* value, due to changes in the peak load voltage, the feedback loop may end up driving the duty cycle over 90%. Even if it is able to regulate a large drop in load voltage, a duty-cycle as high

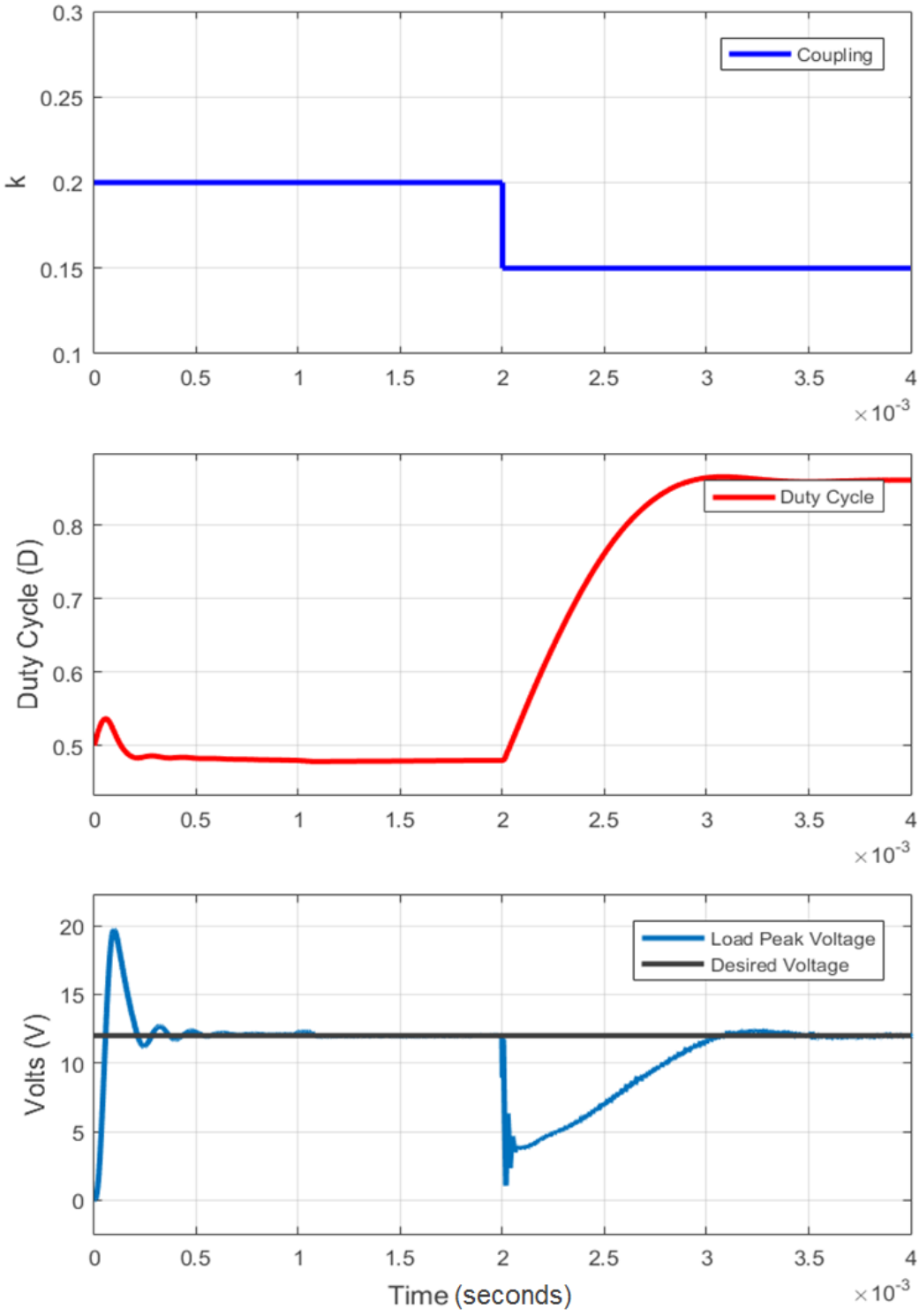

Figure 4.6. Duty cycle increases to 86% in order to compensate drop from $k = 0.2$ to $k = 0.15$.

as 90% would cause the regulation to be inefficient. Figure 4.6 depicts an example of

such case and how the boost converter reacts to large coupling variations.

It can be seen that, for the change in coupling coefficient from 0.2 to 0.15, the duty cycle is driven to a very large value for the compensation process. This of course isn't good for the boost converter due to the increase in conduction loss. Therefore, as a design methodology, the designer should have an idea of the maximum and minimum coupling they're dealing with. Once this maximum is known, the designer can work backwards from the desired load voltage by choosing the proper component values based on equations (13) and (18). The bias duty cycle D should be kept as low as possible. Also, from the simulation result in Figure 4.6, the rise time needed for the load voltage to reach the desired peak is around 1 ms. This time response can be improved by designing more complex and higher order controllers. Overall, further investigation should be done into the proper selection of components and switching topologies for a given coupling constraint. In summary, placing the WPT system under voltage-mode control appears to be a desirable technique for regulating the load peak voltage under coil misalignment. The simulation results show that the DC-DC converter has a significant impact on the open-loop transfer function and that the integral controller does a good job responding to step-like coupling changes.

4.3 Conclusion

In this chapter, a simulation model made using MATLAB/Simulink was built and used validate the proposed concept. The open-loop transfer function was validated via simulation using the sine injection method. An integral controller was added into the model to investigate the WPT system's closed loop performance in regulating the load

voltage. The response of the controller to variations in k showed that using voltage-mode control technique in WPT transfer system is a suitable solution for regulating the load voltage.

Chapter 5

Conclusion and Future Work

WPT is a promising technique for powering biomedical implants, but it still faces several challenging issues such as unstable power delivery due to for example misalignment between the transmitter and receiver coils. Previous work has suggested that the use of negative feedback in the form of transmitter power supply control can be used to regulate the received power [2], [3], [4], [12], [22], [24]. When designing a controller, most of these work did not consider the open-loop transfer function of the power control unit into account. In this Thesis, the open-loop transfer function of the power control unit and the WPT system were taken into account. The system's transfer function was obtained, and accordingly a controller was designed, and its performance was verified through simulation.

In this chapter, we present an overview of the thesis contributions and directions of future work.

5.1 Contributions

The contributions of this thesis are as follows:

a) In Chapter 2 the typical architecture of a WPT system for biomedical implants was presented and discussed. A brief discussion on class-E amplifiers, their operations, and place in a WPT system was presented. Issues related to coil misalignment, such as load voltage variations on the secondary side were

described. A literature review highlighting power supply control techniques to compensate for the effects of coil misalignment was presented.

b) In Chapter 3 a voltage-mode control architecture was presented along with a theoretical derivation of the open-loop system transfer function, which was used to design the controller.

c) In Chapter 4, simulation results were presented and discussed for the open-loop and the closed-loop systems. The analytical, and simulation results based on a Simulink model and using the sine-injection method, were first compared for the open loop system. Next, a Simulink model of the closed-loop system was presented utilizing an integral controller, and the effects of coupling variations were investigated.

5.2 Future work

In derivation of our model for the proposed architecture, it was assumed all inductive elements are ideal and lossless. In practice, this is never the case due to parasitic resistances and capacitances. A more comprehensive model should consider the parasitic elements into account. The controller designed to demonstrate closed-loop control was a first-order integral controller. In order to achieve a better transient response and stability margin, higher order controllers should be investigated. In deriving the analytical equations of an open-loop transfer function, we did not consider the rectifier circuitry and filter capacitors at the receiver end. A more complete model should be considered, taking into account these elements. Once this new model is validated through simulation, the hardware implementation should be carried out.

Bibliography

[1] Jiejian Dai and Daniel C Ludois. A Survey of Wireless Power Transfer and a Critical Comparison of Inductive and Capacitive Coupling for Small Gap Applications. *IEEE Transactions on Power Electronics*, vol. 30, no. 11, pp. 6017-6029, Nov. 2015.

[2] Guoxing Wang, Wentai Liu, Mohanasankar Sivaprakasam, and Gurhan A Kendir. Design and analysis of an adaptive transcutaneous power telemetry for biomedical implants. *IEEE Transactions on Circuits and Systems I: Regular Papers*, vol. 52, no. 10, pp. 2109-2117, Oct. 2005.

[3] HyungGu Park, Joon-Sung Park, YoungGun Pu, Seung-Ok Lim, Yeon-Kuk Moon, Sun-Hee Kim, and Kang-Yoon Lee. A design of high efficiency class-E power amplifier for wireless power transfer system. *Intelligent Radio for Future Personal Terminals (IMWS-IRFPT), 2011 IEEE MTT-S International Microwave Workshop Series on*, Daejeon, 2011, pp. 1-2.

[4] Gouxing Wang, Wentai Liu, Rizwan Bashirullah, Mohanasankar Sivaprakasam, Gurhan A Kendir, Ying Ji, Mark S Humayun, and James D Weiland. A closed loop transcutaneous power transfer system for implantable devices with enhanced stability. *Circuits and Systems, Proceedings of the 2004 International Symposium on,* 2004, pp. IV-17-20 Vol.4.

[5] Fanpeng Kong, Yi Huang, and Laleh Najafizadeh. A coil misalignment compensation concept for wireless power transfer links in biomedical implants. *IEEE Wireless Power Transfer Conference*, 2015, pp. 1–4.

[6] Nathan O Sokal. Class E high-efficiency power amplifiers, from HF to microwave. *Microwave Symposium Digest, 1998 IEEE MTT-S International*, Baltimore, MD, USA, 1998, pp. 1109-1112 vol.2.

[7] Marian Kazimierczuk. Collector amplitude modulation of the class E tuned power amplifier. *IEEE Transactions on Circuits and Systems*, vol. 31, no. 6, pp. 543-549, Jun 1984.

[8] Slobodan I Babic and Cevdet Akyel. Calculating mutual inductance between circular coils with inclined axes in air. *Magnetics, IEEE Transactions on*, 44(7):1743-1750, 2008.

[9] Samer Aldhaher, Patrick C Luk and James F Whidborne. Electronic Tuning of Misaligned Coils in Wireless Power Transfer Systems. *IEEE Transactions on Power Electronics*, vol. 29, no. 11, pp. 5975-5982, Nov. 2014.

[10] Tadashi Suetsugu. Discrete control of class E amplifier with load fluctuation. *2015 IEEE International Telecommunications Energy Conference (INTELEC)*, Osaka, 2015, pp. 1-5.

[11] Samer Aldhaher, Patrick C Luk, Akram Bati and James F Whidborne. Wireless Power Transfer Using Class E Inverter With Saturable DC-Feed Inductor. *IEEE Transactions on Industry Applications*, vol. 50, no. 4, pp. 2710-2718, July-Aug. 2014.

[12] Sun-Han Hwang, Yong-Ho Son and Byung-Jun Jang. Software-based wireless power transfer platform for power control experimentation. *Wireless Power Transfer Conference (WPTC), 2014 IEEE*, Jeju, 2014, pp. 80-83.

[13] *Advantages and Disadvantages in Comparison with Linear Regulator*. Retrieved November 12, 2015, from http://micro.rohm.com/en/techweb/knowledge/dcdc/s-dcdc/02-s-dcdc/2642/

[14] Robert Erickson and Dragan Maksimović. *Fundamentals of power electronics*. Ed. 2, Norwell, Mass.:Kluwer Academics, 2001, pp. 265-330.

[15] David P Kimber. Class e amplifiers and their modulation behavior. Ph.D. dissertation, Electronic, Electrical and Computer Engineering Department, University of Birmingham, Birmingham, UK, 2005.

[16] Dalvir K Saini, Agasthya Ayachit, Marian Kazimierczuk and Hiroo Sekiya. Small-signal analysis of closed-loop PWM boost converter in CCM with complex impedance load. *2016 IEEE International Symposium on Circuits and Systems (ISCAS)*, Montreal, QC, 2016, pp. 433-436.

[17] Robert Erickson and Dragan Maksimović, *Fundamentals of power electronics*. Ed. 2, Norwell, Mass.:Kluwer Academics, 2001, pp. 331-375.

[18] To P Wang, Tsai S Chu and Hai Wu Lee. Wireless power transfer with 6.78-MHz operation frequency on biological media (pork muscle). *2016 IEEE International Symposium on Radio-Frequency Integration Technology (RFIT)*, Taipei, 2016, pp. 1-3.

[19] Hangeok Choi. Practical Feedback Loop Design Considerations for Switched Mode Power Supplies. *Fairchild Semiconductor Power Seminar* (2010 – 2011).

[20] Jian Yin, Deyan Lin, Chi K Lee and S. Y. Ron Hui. Load monitoring and output power control of a wireless power transfer system without any wireless communication

feedback. *2013 IEEE Energy Conversion Congress and Exposition*, Denver, CO, 2013, pp. 4934-4939.

[21] *An Efficiency Primer for Switch-Mode, DC-DC Converter Power Supplies.* Retrieved May 2007, from https://www.maximintegrated.com/en/app-notes/index.mvp/id/4266

[22] P. Si *et al*., "Wireless Power Supply for Implantable Biomedical Device Based on Primary Input Voltage Regulation," *2007 2nd IEEE Conference on Industrial Electronics and Applications*, Harbin, 2007, pp. 235-239.

[23] Luis Andia, Rui-Feng Xue, Kuang-Wei Cheng and Mikyu Je, "Closed loop wireless power transmission for implantable medical devices," *2011 International Symposium on Integrated Circuits*, Singapore, 2011, pp. 404-407.

[24] Dukju Ahn, Seongmin Kim, Jungick Moon and In-Kui Cho, "Wireless Power Transfer With Automatic Feedback Control of Load Resistance Transformation," in *IEEE Transactions on Power Electronics*, vol. 31, no. 11, pp. 7876-7886, Nov. 2016.

[25] Philippe Jourand, Robert Puers, “A Class-E driven inductive power delivery system covering complete upper body,” *Sensor and Actuators A: Physical*, 183 (2012), pp. 132-139

[26] Bert Lenaerts, Robert Puers, “Automatic inductance compensation for class E driven flexible coils” *Sensor and Actuators A: Physical*, 145-146 (2008), pp. 154-160

[27] Kenie Chen and Dimitrios Peroulis, "Design of Highly Efficient Broadband Class-E Power Amplifier Using Synthesized Low-Pass Matching Networks," in *IEEE Transactions on Microwave Theory and Techniques*, vol. 59, no. 12, pp. 3162-3173, Dec. 2011.

[28] Scott D. Kee, Ichiro Aoki, Ali Hajimiri and David Rutledge, "The class-E/F family of ZVS switching amplifiers," in *IEEE Transactions on Microwave Theory and Techniques*, vol. 51, no. 6, pp. 1677-1690, June 2003.